HHS Public Access

Author manuscript

Circ Res. Author manuscript; available in PMC 2020 March 15.

Published in final edited form as:

Circ Res. 2019 March 15; 124(6): 881–890. doi:10.1161/CIRCRESAHA.118.314030.

Molecular Imaging Visualizes Recruitment of Inflammatory Monocytes and Macrophages to the Injured Heart

Gyu Seong Heo[1], **Benjamin Kopecky**[2], **Deborah Sultan**[1], **Monica Ou**[3], **Guoshuai Feng**[2], **Geetika Bajpai**[2], **Xiaohui Zhang**[1], **Hannah Luehmann**[1], **Lisa Detering**[1], **Yi Su**[1], **Florian Leuschner**[4], **Christophe Combadière**[5], **Daniel Kreisel**[6,8], **Robert J. Gropler**[1], **Steven L. Brody**[2], **Yongjian Liu**[1,*], and **Kory J. Lavine**[2,7,8,*]

[1]Department of Radiology, Washington University School of Medicine, St. Louis, MO USA;

[2]Department of Medicine, Washington University School of Medicine, St. Louis, MO USA;

[3]Department of Biology, Saint Louis University, St. Louis, MO USA;

[4]Department of Internal Medicine III, University of Heidelberg, Heidelberg, Germany;

[5]Sorbonne Université, Inserm, CNRS, Centre d'immunologie et des maladies infectieuses, Cimi-Paris, F-75013 Paris, France;

[6]Department of Surgery, Washington University School of Medicine, St. Louis, MO USA;

[7]Department of Developmental Biology, Washington University School of Medicine, St. Louis, MO USA;

[8]Department of Immunology and Pathology, Washington University School of Medicine, St. Louis, MO USA.

Abstract

Rationale: Paradigm shifting studies have revealed that the heart contains functionally diverse populations of macrophages derived from distinct embryonic and adult hematopoietic progenitors. Under steady state conditions, the heart is largely populated by CCR2- macrophages of embryonic descent. Following tissue injury, a dramatic shift in macrophage composition occurs whereby CCR2+ monocytes are recruited to the heart and differentiate into inflammatory CCR2+ macrophages that contribute to heart failure progression. Currently, there are no techniques to

Address correspondence to: Dr. Kory J. Lavine, Division of Cardiology, Department of Medicine, 660 South Euclid, Campus Box 8086, St. Louis, MO 63110, Tel: 314 362-1171, klavine@wustl.edu, Dr. Yongjian Liu, Department of Radiology, 510 S. Kingshighway Blvd, Campus Box 8225, St. Louis, MO 63110, Tel: 314 362-8431, yongjianliu@wustl.edu.

AUTHOR CONTRIBUTIONS

K.J. Lavine and Y. Liu designed and supervised the project. G.S. Heo, B. Kopecky, M. Ou, G. Feng, G. Bajpai, D. Sultan, X. Zhang, H. Luehmann, L. Detering, and Y. Su performed the experiments and analyzed the data. F. Leuschner provided human ischemic cardiomyopathy specimens. Y. Liu and K.J. Lavine wrote and edited the manuscript. D. Kreisel, R.J. Gropler, C. Combadiere, S.L. Brody, K.J. Lavine and Y. Liu edited the manuscript.

*Co-senior authors

In December 2018, the average time from submission to first decision for all original research papers submitted to *Circulation Research* was 14.99 days.

DISCLOSURES

Yongjian Liu, Daniel Kreisel, Christophe Combadiere, Robert Gropler, Steven Brody, and Kory Lavine have a pending patent entitled "Compositions and methods for detecting CCR2 receptors" (application number 15/611,577).

noninvasively detect CCR2+ monocyte recruitment into the heart and thus identify patients who may be candidates for immunomodulatory therapy.

Objective: To develop a noninvasive molecular imaging strategy with high sensitivity and specificity to visualize inflammatory monocyte and macrophage accumulation in the heart.

Methods and Results: We synthesized and tested the performance of a positron emission tomography (PET) radiotracer (^{68}Ga-DOTA-ECL1i) that allosterically binds to CCR2. In naïve mice, the radiotracer was quickly cleared from the blood and displayed minimal retention in major organs. In contrast, biodistribution and PET demonstrated strong myocardial tracer uptake in 2 models of cardiac injury (diphtheria toxin induced cardiomyocyte ablation and reperfused myocardial infarction). ^{68}Ga-DOTA-ECL1i signal localized to sites of tissue injury and was independent of blood pool activity as assessed by quantitative PET and *ex vivo* autoradiography. ^{68}Ga-DOTA-ECL1i uptake was associated with CCR2+ monocyte and CCR2+ macrophage infiltration into the heart and was abrogated in CCR2$^{-/-}$ mice, demonstrating target specificity. Autoradiography demonstrated that ^{68}Ga-DOTA-ECL1i specifically binds human heart failure specimens and with signal intensity associated with CCR2+ macrophage abundance.

Conclusions: These findings demonstrate the sensitivity and specificity of ^{68}Ga-DOTA-ECL1i in the mouse heart and highlight the translational potential of this agent to noninvasively visualize CCR2+ monocyte recruitment and inflammatory macrophage accumulation in patients.

Subject Terms:

Inflammation; Ischemia; Translational Studies

Keywords

CCR2; positron emission tomography; myocardial infarction; monocytes; macrophages; molecular imaging; chemokine; myocardial inflammation

INTRODUCTION

It is increasingly recognized that the innate immune system is robustly activated at the local and systemic level following ischemic myocardial injury.[1] From a prognostic standpoint, the intensity and duration of inflammation following a myocardial infarction (MI) is strongly associated with clinical outcomes. For example, despite similar infarct sizes, patients who display greater extents of inflammation experience accelerated post-infarct remodeling, left ventricle (LV) systolic dysfunction, and higher mortality rates.[2–4] Previous studies utilizing human pathological specimens and animal models of MI and ischemia reperfusion injury have demonstrated that monocytes, macrophages, and neutrophils accumulate within the injured myocardium and constitute the initial inflammatory responses to cardiac injury.[5, 6]

While it is well established that neutrophils produce significant inflammatory and oxidative responses and contribute to the development of heart failure, considerable debate exists regarding the exact role of monocytes and macrophages within the injured heart. In fact, there are numerous examples of contradictory reports claiming that monocytes and macrophages are both harmful following injury and are essential mediators of tissue repair.[7]

Macrophages within the infarcted heart not only drive vigorous inflammatory responses and LV remodeling, but also are required for the resolution of inflammation and reparative activities including angiogenesis.[8] One proposed explanation for these findings is that distinct macrophage populations may mediate inflammatory and reparative macrophage behaviors.[9] However, the exact identities, origins, and functions of these proposed macrophage subsets have remained elusive.

Recently, we have uncovered a previously unrecognized complexity within the innate immune system that begins to reconcile conflicting observations that inflammation is paradoxically both harmful following cardiac injury and essential for myocardial repair. Using a combination of genetic lineage tracing, flow cytometry, and immunostaining, we have demonstrated that the mouse and human hearts contain a complex and heterogeneous array of resident and recruited macrophage subsets derived from embryonic and adult hematopoietic progenitors with differing recruitment dynamics and functions.[10] Under steady state conditions, the heart contains at least 2 functionally distinct macrophage subsets: CCR2- and CCR2+ macrophages. Resident CCR2- macrophages are derived from embryonic progenitors (yolk sac and fetal liver) and are maintained locally independent of blood monocyte input.[10] In contrast, CCR2+ macrophages are derived from adult bone marrow progenitors and are continually replenished by blood monocytes. Resident CCR2- macrophages are critical regulators of coronary development, vascular expansion, and tissue repair.[11, 12]

Following myocardial infarction, a dramatic shift in macrophage composition and ontogeny is observed. Ly6C^{high}, CCR2+ monocytes infiltrate the heart, replace resident cardiac macrophage subsets, and differentiate into CCR2+ macrophages to stimulate pro-inflammatory responses, collateral tissue damage, and ultimately contribute to heart failure pathogenesis.[11] These findings implicate infiltrating CCR2+ monocytes and macrophages as important mediators of heart failure pathogenesis and suggest that therapies which target these cells may improve outcomes for patients who suffer a myocardial infarction.

Current techniques to detect CCR2+ monocyte and macrophage accumulation within the heart are limited to pathological analyses of myocardial tissue, which is clinically impractical. To date, no noninvasive approaches exist to image CCR2+ monocytes and macrophages in intact animals in real time. We have recently described the use of a peptide-based radiotracer that binds to the extracellular domain of CCR2 (ECL1i) for noninvasive imaging of inflammation using positron emission tomography (PET).[13–17] The ^{64}Cu-DOTA-ECL1i tracer specifically detects CCR2+ monocyte and macrophage accumulation within the lung following ischemia reperfusion injury and lipopolysaccharide administration. While this imaging tool proved to be effective in animal models, the production of ^{64}Cu needs cyclotron facility and the relatively long half-life of ^{64}Cu ($t_{1/2}$= 12.7 h) precludes serial imaging in an acute setting and increases the concerns of radiation exposure.

To mitigate this issue, we developed a gallium-68 radiolabeled CCR2 PET tracer (^{68}Ga-DOTA-ECL1i) with a relatively short half-life ($t_{1/2}$= 68 min) that can be produced using a commercially available ^{68}Ge/^{68}Ga generator. The ^{68}Ga-DOTA-ECL1i tracer represents an ideal tool for serial imaging of CCR2+ monocyte recruitment and inflammatory macrophage

accumulation with reduced radiation exposure. We show that implementation of the ^{68}Ga-DOTA-ECL1i radiotracer in vivo detected regions of myocardial injury in mouse models in a CCR2+ monocyte and macrophage specific fashion, and the same cell populations in *ex vivo* diseased human cardiac tissue using autoradiography. Together, these findings establish sensitivity and specificity of ^{68}Ga-DOTA-ECL1i in the mouse and human hearts and support the use of this imaging agent to noninvasively and dynamically visualize inflammatory monocyte and macrophage recruitment.

METHODS

The authors declare that all supporting data are available within the article and its online supplementary files. Raw data are available from the corresponding author upon reasonable request.

Detailed descriptions of mouse strains, ^{68}Ga-DOTA-ECL1i synthesis, biodistribution, autoradiography, PET/CT, reperfused myocardial infarction, DT cardiomyocyte ablation, echocardiography, flow cytometry, immunostaining, RT-PCR, and statistical analysis are provided in the online supplement.

RESULTS

^{68}Ga-DOTA-ECL1i displays rapid in vivo pharmacokinetics and is retained in the heart following sterile tissue injury.

^{68}Ga-DOTA-ECL1i was synthesized following the radiosynthetic route outlined in Figure 1A. High yield and specific activity (6.05 MBq/nmol) were obtained enabling administration of small quantities (0.92 nmol/mouse) for in vivo imaging. Radiochemical purity (≥95%) of the tracer was demonstrated by radio-HPLC prior to in vitro and in vivo applications. Stability studies demonstrated that the tracer remained intact in mouse serum for up to 4 hours (Figure 1B). To decipher whether ^{68}Ga-DOTA-ECL1i could selectively detect CCR2+ monocytes and macrophages recruited to the injured heart, we first utilized a cardiomyocyte ablation model. Transgenic mice were generated that expressed the Diphtheria toxin receptor (DTR) under the control of the rat Troponin T2 (Tnnt2) promotor. We used a modified version of the DTR (human HB-EGF I117V/L148V) that lacks capacity to signal *via* epidermal growth factor receptor but retains sensitivity to Diphtheria toxin (DT).[18] Tnnt2-DTR mice specifically express DTR in cardiomyocytes and display evidence of cardiomyocyte cell death following administration of DT (25 ng IP) (Online Figure I).

Similar to previous studies employing DT-mediated cardiomyocyte ablation systems, injection of DT (25 ng IP) resulted in marked accumulation of CCR2+ monocytes and macrophages in the heart, compared to littermate controls (Figure 1C).[11] In vivo biodistribution analysis performed 4 days following DT administration revealed rapid renal clearance and low organ retention of ^{68}Ga-DOTA-ECL1i at 1 hour post tail vein injection in DT treated wildtype (WT+DT) mice. Increased tracer retention was observed in most major organs including blood, liver, spleen, heart and marrow beginning at day 3 following DT injection. By day 4 there was a nearly a 10-fold increase of myocardial radioactivity between the WT+DT and Tnnt2-DTR+DT groups ($p<0.001$, n=6–8/group). Increased ^{68}Ga-

DOTA-ECL1i retention was also observed outside of the myocardium including in the blood, lung, liver, spleen, muscle, bone marrow, and stomach, possibly as a result of extramedullary myelopoiesis, venous congestion, and/or systemic hypoperfusion (Figure 1D).[19–22] Immunostaining revealed increased abundance of CCR2+ cells in the spleen and lung (Online Figure. II). As the liver did not contain elevated numbers of CCR2+ cells, observed increases in liver ^{68}Ga-DOTA-ECL1i retention in Tnnt2-DTR mice may be a result of expanded blood pool as a result of severe biventricular heart failure and venous congestion. Importantly, Tnnt2-DTR/CCR2 KO mice treated with DT did not demonstrate significant increases in ^{68}Ga-DOTA-ECL1i retention compared to WT+DT mice establishing tracer specificity. We further compared heart/blood and heart/muscle uptake ratios to address the potential contribution of non-specific blood pool radiotracer retention. Tnnt2-DTR+DT mice displayed significantly increased heart/blood and heart/muscle uptake ratios compared to WT+DT and Tnnt2-DTR/CCR2 KO+DT mice, indicating selective accumulation of ^{68}Ga-DOTA-ECL1i in the heart over the blood pool (Figure 1E).

^{68}Ga-DOTA-ECL1i is suitable for PET and readily detects cardiac inflammation in a DT cardiomyocyte injury model.

We next examined the suitability of ^{68}Ga-DOTA-ECL1i for in vivo PET of CCR2+ monocyte and macrophage accumulation in the heart using our DT cardiomyocyte injury mouse model. PET images (40–60 minutes summed images) revealed intense and heterogeneous PET signal in the hearts of Tnnt2-DTR+DT mice (Figure 2A). In comparison, minimal PET signal was observed in the hearts of WT, WT+DT, or Tnnt2-DTR mice. Quantitative analysis demonstrated approximately 7 times higher PET signal in the hearts of Tnnt2-DTR mice compared to the other groups (Figure 2B), consistent with the biodistribution analysis. We then compared heart/aorta uptake ratios between experimental groups to normalize the effect of tracer blood pool retention. Tnnt2-DTR+DT mice showed significantly higher tracer uptake ratios compared to controls ($p<0.05$, $n=4$), indicating that while blood pool signal was evident, ^{68}Ga-DOTA-ECL1i effectively labeled cells within the injured heart (Figure 2C). To verify the presence of ^{68}Ga-DOTA-ECL1i signal within the myocardium, hearts were collected immediately after PET and slices prepared for *ex vivo* autoradiography. In agreement with PET, the summed radioactive counts in Tnnt2-DTR+DT hearts were significantly elevated compared to control hearts (Figure 2D, E). Measurement of Il1β, Ccl2, and Il6 mRNA expression further revealed that ^{68}Ga-DOTA-ECL1i signal closely correlated with inflammatory chemokine and cytokine expression in Tnnt2-DTR +DT hearts (Figure 2F). Taken together, these data demonstrate the suitability of ^{68}Ga-DOTA-ECL1i for PET and establish the ability of ^{68}Ga-DOTA-ECL1i to identify myocardial CCR2+ monocyte and macrophage accumulation in our DT cardiomyocyte injury model.

Serial noninvasive ^{68}Ga-DOTA-ECL1i PET effectively detects CCR2+ monocytes and macrophages within the infarct region following ischemia reperfusion injury.

To further assess the sensitivity and specificity of ^{68}Ga-DOTA-ECL1i to detect CCR2+ monocytes and macrophages within the injured heart, we performed serial PET in an ischemia reperfusion injury mouse model. We employed a closed-chest ischemia reperfusion system to minimize confounding effects of inflammation associated with thoracotomy.[23] We

utilized ^{18}F-FDG PET/CT to noninvasively identify the infarct area. Consistent with ischemia reperfusion injury involving the left coronary artery, ^{18}F-FDG PET/CT demonstrated evidence of an anterior and apical infarct (Figure 3A), which was also confirmed by polar map analysis (Online Figure IIIA). Quantification of PET signal showed comparable ^{18}F-FDG heart uptake among the MI mice, sham-operated mice, and naïve animals during the longitudinal study (Online Figure IIIB), consistent with a previous report.[24]

^{68}Ga-DOTA-ECL1i PET/CT obtained on day 4 following ischemia reperfusion injury revealed high PET signal localized to the infarct region. In contrast, minimal PET signal was detected in the hearts of sham-operated mice (Figure 3A–B). Quantitative serial PET analysis performed on days 1, 4, 7, 14, and 21 following ischemia reperfusion injury demonstrated highest PET signal 4 days following ischemia reperfusion injury (Figure 3C). At this time point, there was a statistically significant increase in total PET signal between the hearts of mice that underwent the sham operation versus ischemia reperfusion injury. PET of CCR2$^{-/-}$ mice 4 days following ischemia reperfusion injury showed no increase in tracer uptake compared to either sham operated or naïve mice, demonstrating the specificity of ^{68}Ga-DOTA-ECL1i detecting CCR2+ cells. Moreover, quantification of infarct/remote tracer uptake ratios throughout the above time course revealed statistically significant increases in PET signal intensity on days 4 and 7 following ischemia reperfusion injury ($p<0.01$ and $p<0.001$, respectively), with peak PET signal intensity observed on day 4 following ischemia reperfusion injury (Figure 3D). Biodistribution at day 4 post ischemia reperfusion injury (Figure 3E) showed robust tracer retention in the heart. Minimal blood retention was evident within this model as blood signal was not increased compared to that measured in WT+DT mice (Figure 1D). Histology, flow cytometry, and immunostaining confirmed that inflammatory cell accumulation and CCR2+ monocyte (CCR2+MHC-II^{low}) and CCR2+ macrophage (CCR2+MHC-II^{low}) abundance within the infarct area was greatest 4 days post ischemia reperfusion injury and gradually reduced thereafter in our closed-chest model (Fig. 3F–H).

Importantly, the blood pool retention of ^{68}Ga-DOTA-ECL1i measured by aortic PET signal showed no statistically significant difference between sham operated and ischemia reperfusion groups (Online Figure IIIC). Furthermore, aortic PET signal intensity was more than 2-fold lower than PET signal intensity measured within the heart, strongly suggesting that ^{68}Ga-DOTA-ECL1i accumulated within the infarcted myocardial tissue. Consistent with this interpretation, *ex vivo* autoradiography performed 4 days after ischemia reperfusion injury revealed significantly increased radioactive signal within the heart compared to sham operated controls (Online Figure IIID, E). These data demonstrate the ability of ^{68}Ga-DOTA-ECL1i to specifically detect CCR2+ monocyte and macrophage accumulation within and around the infarct region following ischemia reperfusion injury and highlight the feasibility of serial PET at acute setting using this radiotracer.

To assess the predictive value of ^{68}Ga-DOTA-ECL1i imaging, we examined whether ^{68}Ga-DOTA-ECL1i signal intensity measured by PET on day 4 post ischemia reperfusion injury was associated with LV function and infarct size measured by echocardiography 28 days following ischemia reperfusion injury. Remarkably, ^{68}Ga-DOTA-ECL1i signal was

predictive of both LV ejection fraction and akinetic area. Mice that displayed higher ^{68}Ga-DOTA-ECL1i signal intensity demonstrated lower LV ejection fraction and larger akinetic area (Figure 3I). These observations highlight the potential clinical utility of imaging CCR2+ monocyte and macrophage accumulation following myocardial infarction.

^{68}Ga-DOTA-ECL1i detects CCR2+ monocytes and macrophages in the human heart.

We next assessed the capability of ^{68}Ga-DOTA-ECL1i to detect CCR2+ monocytes and macrophages within the *ex vivo* human heart using autoradiography.[15] We focused our studies on tissues obtained from patients with recent myocardial infarction or ischemic cardiomyopathy (n=16) (Online Table I). ^{68}Ga-DOTA-ECL1i autoradiography demonstrated heterogeneous radioactive signal in specimens obtained from individuals with acute myocardial infarction and chronic ischemic cardiomyopathy (Figure 4A). Addition of excess nonradioactive DOTA-ECL1i in the ischemic cardiomyopathic samples led to a significant reduction in measured radioactive signal indicating specificity of probe binding (Figure 4B). To assess whether the extent of ^{68}Ga-DOTA-ECL1i binding was associated with CCR2+ monocyte and macrophage abundance, we performed immunohistochemistry for CD68 (monocyte and macrophage marker) and CCR2. We then quantified the number of CCR2-, CD68+ and CCR2+, and CD68+ cells present within the human heart failure specimens evaluated by autoradiography (Figure 4C). Linear regression analysis revealed that ^{68}Ga-DOTA-ECL1i signal intensity was associated with total number of CD68+ monocytes and macrophages detected by immunostaining ($p=0.010$, $r^2=0.387$). Consistent with the ability of ^{68}Ga-DOTA-ECL1i to specifically recognize CCR2, ^{68}Ga-DOTA-ECL1i signal intensity was associated with CCR2+, CD68+ cell abundance ($p=0.0023$, $r^2=0.498$). No relationship was evident between ^{68}Ga-DOTA-ECL1i signal intensity and CCR2-, CD68+ cell abundance ($p=0.32$, $r^2=0.069$) (Figure 4D). The data suggest that ^{68}Ga-DOTA-ECL1i likely recognizes CCR2+ monocytes and macrophages in human cardiac tissue and highlight the potential applicability of using ^{68}Ga-DOTA-ECL1i to image CCR2+ monocyte and macrophage accumulation in acute myocardial infarction and heart failure patients.

DISCUSSION

Despite the development and implementation of advanced imaging techniques and reagents, it remains challenging to gather precise information regarding prognosis for patients who suffered an acute myocardial infarction or those with heart failure[25–31]. Numerous studies across a spectrum of cardiovascular diseases have unveiled important roles for innate immunity in disease pathogenesis.[25, 32] Likewise, biomarkers of inflammation have been shown to predict clinical outcomes in the context of heart failure and atherosclerosis.[33, 34] Investigation of a strategy to inhibit IL1β signaling described in the CANTOS trial established the principle that inflammation is a relevant therapeutic target, reducing the incidence of atherosclerotic events in a high risk population.[35, 36] However, the precise immune cell populations that drive inflammatory responses in the heart and vasculature have remained elusive.

Recently, we and others have identified functionally distinct macrophage populations that reside within the mouse and human heart under steady state and diseased conditions.

[10, 11, 12, 37] Among these populations, CCR2+ macrophages represent a particularly pro-inflammatory subset derived from circulating monocytes. In the setting of cardiac tissue injury, CCR2+ monocytes are recruited to the heart in large numbers, differentiate into CCR2+ macrophages, and promote collateral tissue injury through the generation of inflammatory cytokines/chemokines (i.e., IL1β), recruitment of neutrophils and additional monocytes, and production of oxidative species. Inhibition of CCR2+ monocyte and macrophage accumulation in the injured heart is sufficient to reduce inflammation and improve outcomes, highlighting the potential utility of therapeutics that target these cell populations.

Based on these findings, we developed a peptide-based PET tracer (^{68}Ga-DOTA-ECL1i) to noninvasively track the recruitment, accumulation, and resolution of CCR2+ monocytes and macrophages. Our previous studies have established that ECL1i binds to an allosteric position within the CCR2 protein and that ECL1i-CCR2 binding is selectively increased in the presence of a CCR2 ligand (CCL2 or CCL7).[13–17] Compared to our previously described ^{64}Cu-DOTA-ECL1i imaging probe, ^{68}Ga-DOTA-ECL1i tracer has a number of unique properties to further broaden CCR2 imaging research, including the short half-life of ^{68}Ga for reduced radiation exposure, positive charge facilitating rapid clearance, commercially available ^{68}Ge/^{68}Ga generator for multiple dose preparations and serial imaging in the acute setting, and low liver retention for hepatic imaging.[15]

Using two mouse models of cardiac injury, we revealed that ^{68}Ga-DOTA-ECL1i PET specifically detects the accumulation of CCR2+ monocytes and macrophages in the injured myocardium. Concomitant ^{18}F-FDG PET demonstrated that ^{68}Ga-DOTA-ECL1i specifically localized inflammation to the infarct and peri-infarct area. In addition, we showed that the short radioactive half-life of ^{68}Ga-DOTA-ECL1i was sufficient to support serial imaging applications. Finally, we provided evidence that ^{68}Ga-DOTA-ECL1i recognizes human CCR2+ monocytes and macrophages within tissue specimens obtained from patients who either experienced a myocardial infarction or were diagnosed with chronic ischemic cardiomyopathy. Compared to other reported molecular imaging probes detecting myocardial inflammation after ischemia,[38] our ^{68}Ga-DOTA-ECL1i probe not only showed close correlation to inflammatory biomarkers, but also demonstrated its predictive value in monitoring LV function and extent of infarction. Thus, these findings establish the applicability of ^{68}Ga-DOTA-ECL1i PET in mouse models and suggest that ^{68}Ga-DOTA-ECL1i may similarly be suitable to noninvasively visualize CCR2+ monocyte and CCR2+ macrophage recruitment in humans.

Surprisingly little is understood regarding the exact timing, patient to patient heterogeneity, and prognostic relevance of monocyte recruitment, macrophage accumulation, and inflammatory cell resolution following myocardial infarction in humans. ^{68}Ga-DOTA-ECL1i PET (in conjunction with MRI or CT) would provide new and important insights into these questions as they relate to CCR2+ monocytes and macrophages. Most importantly, ^{68}Ga-DOTA-ECL1i imaging has the clinical potential to identify patients best served by immunomodulatory therapy, based on the presence of exaggerated or prolonged inflammatory responses in the heart. Future clinical studies will be required to address these important issues and questions.

In the present study, we focused on mouse models of sterile tissue injury, including DT cardiomyocyte ablation and ischemic reperfusion injury. Whether ^{68}Ga-DOTA-ECL1i PET identifies inflammatory responses in mouse models of other cardiac diseases such as myocarditis, pressure overload, and toxin exposures, remains to be evaluated. An important limitation of ^{68}Ga-DOTA-ECL1i is that it may recognize immune cells other than monocytes and macrophages (i.e., dendritic cells or lymphocytes) that express CCR2. For example, dendritic cells have been shown to infiltrate the heart following myocardial injury including myocarditis, albeit at significantly lower numbers compared to macrophages.[39] Therefore, a precise understanding of immune composition is essential to interpret the likely cell specificity of ^{68}Ga-DOTA-ECL1i PET. An additional limitation is that *ex vivo* autoradiography of human cardiac tissue specimens does not guarantee similar performance of ^{68}Ga-DOTA-ECL1i in living patients. Proof of concept human studies will undoubtedly be required to establish the potential use of ^{68}Ga-DOTA-ECL1i in patients with cardiovascular disease.

In conclusion, we have generated a peptide-based radiotracer (^{68}Ga-DOTA-ECL1i) that specifically recognizes CCR2+ monocytes and macrophages and demonstrated the suitability of ^{68}Ga-DOTA-ECL1i PET to serially visualize recruitment of CCR2+ monocytes and macrophages to the heart in intact animals. Collectively, these findings support future assessment of this tracer to noninvasively image myocardial inflammation in humans.

Supplementary Material

Refer to Web version on PubMed Central for supplementary material.

ACKNOWLEDGMENTS

We thank the small animal imaging facility and cyclotron facility at Washington University for assistance with this research and Drs. Bin Zho and Kenji Kohno for providing the rat Tnnt2 promotor and human HB-EGF (I117V/L148V) constructs. We acknowledge the Mouse Genetics Core at Washington University for assistance in generating Tnnt2-DTR transgenic mice.

SOURCES OF FUNDING

K.J.L. is supported by the National Institutes of Health (NIH) K08 HL123519, R01 HL138466, R01 HL139714, Burroughs Welcome Fund (1014782), Children's Discovery Institute of Washington University and St. Louis Children's Hospital (CH-II-2015-462, CH-II-2017-628), and Foundation of Barnes-Jewish Hospital (8038–88). Y.L. is supported by NIH R01 HL125655 and HL131908. DK is supported by 1P01AI116501, R01 HL094601, Veterans Administration Merit Review grant 1I01BX002730 and The Foundation for Barnes-Jewish Hospital. SLB is the Dorothy R and Hubert C Moog Professor of Pulmonary Medicine, awarded through the Barnes-Jewish Hospital Foundation.

Nonstandard Abbreviations and Acronyms:

^{18}F-FDG	^{18}F- Fluorodeoxyglucose
^{64}Cu	^{64}Copper
^{68}Ga	^{68}Gallium
CCR2	C-C chemokine receptor type 2

DOTA	1,4,7,10-Tetraazacyclododecane-1,4,7,10-tetraacetic acid
ECL1i	extracellular loop 1 inverso
HPLC	high performance liquid chromatography
LV	left ventricle
MI	myocardial infarction
PET/CT	positron emission tomography/computed tomography

REFERENCES

1. Libby P, Nahrendorf M, Swirski FK. Leukocytes link local and systemic inflammation in ischemic cardiovascular disease: An expanded “cardiovascular continuum”. J Am Coll Cardiol. 2016;67:1091–1103 [PubMed: 26940931]
2. Wrigley BJ, Shantsila E, Tapp LD, Lip GY. Cd14++cd16+ monocytes in patients with acute ischaemic heart failure. Eur J Clin Invest. 2013;43:121–130 [PubMed: 23240665]
3. Zhou X, Liu XL, Ji WJ, Liu JX, Guo ZZ, Ren D, Ma YQ, Zeng S, Xu ZW, Li HX, Wang PP, Zhang Z, Li YM, Benefield BC, Zawada AM, Thorp EB, Lee DC, Heine GH. The kinetics of circulating monocyte subsets and monocyte-platelet aggregates in the acute phase of st-elevation myocardial infarction: Associations with 2-year cardiovascular events. Medicine (Baltimore). 2016;95:e3466 [PubMed: 27149446]
4. Lu W, Zhang Z, Fu C, Ma G. Intermediate monocytes lead to enhanced myocardial remodelling in stemi patients with diabetes. Int Heart J. 2015;56:22–28 [PubMed: 25503660]
5. Shinagawa H, Frantz S. Cellular immunity and cardiac remodeling after myocardial infarction: Role of neutrophils, monocytes, and macrophages. Curr Heart Fail Rep. 2015;12:247–254 [PubMed: 25721354]
6. Swirski FK. Inflammation and repair in the ischaemic myocardium. Hamostaseologie. 2015;35:34–36 [PubMed: 25375277]
7. Glaros T, Larsen M, Li L. Macrophages and fibroblasts during inflammation, tissue damage and organ injury. Front Biosci (Landmark Ed). 2009;14:3988–3993 [PubMed: 19273328]
8. Frantz S, Nahrendorf M. Cardiac macrophages and their role in ischaemic heart disease. Cardiovasc Res. 2014;102:240–248 [PubMed: 24501331]
9. Nahrendorf M, Swirski FK, Aikawa E, Stangenberg L, Wurdinger T, Figueiredo JL, Libby P, Weissleder R, Pittet MJ. The healing myocardium sequentially mobilizes two monocyte subsets with divergent and complementary functions. J Exp Med. 2007;204:3037–3047 [PubMed: 18025128]
10. Epelman S, Lavine KJ, Beaudin AE, Sojka DK, Carrero JA, Calderon B, Brija T, Gautier EL, Ivanov S, Satpathy AT, Schilling JD, Schwendener R, Sergin I, Razani B, Forsberg EC, Yokoyama WM, Unanue ER, Colonna M, Randolph GJ, Mann DL. Embryonic and adult-derived resident cardiac macrophages are maintained through distinct mechanisms at steady state and during inflammation. Immunity. 2014;40:91–104 [PubMed: 24439267]
11. Lavine KJ, Epelman S, Uchida K, Weber KJ, Nichols CG, Schilling JD, Ornitz DM, Randolph GJ, Mann DL. Distinct macrophage lineages contribute to disparate patterns of cardiac recovery and remodeling in the neonatal and adult heart. Proc Natl Acad Sci U S A. 2014;111:16029–16034 [PubMed: 25349429]
12. Leid J, Carrelha J, Boukarabila H, Epelman S, Jacobsen SE, Lavine KJ. Primitive embryonic macrophages are required for coronary development and maturation. Circ Res. 2016;118:1498–1511 [PubMed: 27009605]
13. Li W, Luehmann HP, Hsiao HM, Tanaka S, Higashikubo R, Gauthier JM, Sultan D, Lavine KJ, Brody SL, Gelman AE, Gropler RJ, Liu Y, Kreisel D. Visualization of monocytic cells in regressing atherosclerotic plaques by intravital 2-photon and positron emission tomography-based imaging. Arterioscler Thromb Vasc Biol. 2018;38:1030–1036 [PubMed: 29567678]

14. Williams JW, Elvington A, Ivanov S, Kessler S, Luehmann H, Baba O, Saunders BT, Kim KW, Johnson MW, Craft CS, Choi JH, Sorci-Thomas MG, Zinselmeyer BH, Brestoff JR, Liu Y, Randolph GJ. Thermoneutrality but not ucp1 deficiency suppresses monocyte mobilization into blood. Circ Res. 2017;121:662–676 [PubMed: 28696252]
15. Liu Y, Gunsten SP, Sultan DH, Luehmann HP, Zhao Y, Blackwell TS, Bollermann-Nowlis Z, Pan JH, Byers DE, Atkinson JJ, Kreisel D, Holtzman MJ, Gropler RJ, Combadiere C, Brody SL. Pet-based imaging of chemokine receptor 2 in experimental and disease-related lung inflammation. Radiology. 2017;283:758–768 [PubMed: 28045644]
16. Liu Y, Li W, Luehmann HP, Zhao Y, Detering L, Sultan DH, Hsiao HM, Krupnick AS, Gelman AE, Combadiere C, Gropler RJ, Brody SL, Kreisel D. Noninvasive imaging of ccr2(+) cells in ischemia-reperfusion injury after lung transplantation. Am J Transplant. 2016;16:3016–3023 [PubMed: 27273836]
17. Auvynet C, Baudesson de Chanville C, Hermand P, Dorgham K, Piesse C, Pouchy C, Carlier L, Poupel L, Barthelemy S, Felouzis V, Lacombe C, Sagan S, Chemtob S, Quiniou C, Salomon B, Deterre P, Sennlaub F, Combadiere C. Ecl1i, d(lgtflkc), a novel, small peptide that specifically inhibits ccl2-dependent migration. Faseb j. 2016;30:2370–2381 [PubMed: 26979087]
18. Furukawa N, Saito M, Hakoshima T, Kohno K. A diphtheria toxin receptor deficient in epidermal growth factor-like biological activity. J Biochem. 2006;140:831–841 [PubMed: 17071947]
19. Leuschner F, Rauch PJ, Ueno T, Gorbatov R, Marinelli B, Lee WW, Dutta P, Wei Y, Robbins C, Iwamoto Y, Sena B, Chudnovskiy A, Panizzi P, Keliher E, Higgins JM, Libby P, Moskowitz MA, Pittet MJ, Swirski FK, Weissleder R, Nahrendorf M. Rapid monocyte kinetics in acute myocardial infarction are sustained by extramedullary monocytopoiesis. J Exp Med. 2012;209:123–137 [PubMed: 22213805]
20. Dutta P, Sager HB, Stengel KR, Naxerova K, Courties G, Saez B, Silberstein L, Heidt T, Sebas M, Sun Y, Wojtkiewicz G, Feruglio PF, King K, Baker JN, van der Laan AM, Borodovsky A, Fitzgerald K, Hulsmans M, Hoyer F, Iwamoto Y, Vinegoni C, Brown D, Di Carli M, Libby P, Hiebert SW, Scadden DT, Swirski FK, Weissleder R, Nahrendorf M. Myocardial infarction activates ccr2(+) hematopoietic stem and progenitor cells. Cell Stem Cell. 2015;16:477–487 [PubMed: 25957903]
21. Robbins CS, Chudnovskiy A, Rauch PJ, Figueiredo JL, Iwamoto Y, Gorbatov R, Etzrodt M, Weber GF, Ueno T, van Rooijen N, Mulligan-Kehoe MJ, Libby P, Nahrendorf M, Pittet MJ, Weissleder R, Swirski FK. Extramedullary hematopoiesis generates ly-6c(high) monocytes that infiltrate atherosclerotic lesions. Circulation. 2012;125:364–374 [PubMed: 22144566]
22. Dutta P, Courties G, Wei Y, Leuschner F, Gorbatov R, Robbins CS, Iwamoto Y, Thompson B, Carlson AL, Heidt T, Majmudar MD, Lasitschka F, Etzrodt M, Waterman P, Waring MT, Chicoine AT, van der Laan AM, Niessen HW, Piek JJ, Rubin BB, Butany J, Stone JR, Katus HA, Murphy SA, Morrow DA, Sabatine MS, Vinegoni C, Moskowitz MA, Pittet MJ, Libby P, Lin CP, Swirski FK, Weissleder R, Nahrendorf M. Myocardial infarction accelerates atherosclerosis. Nature. 2012;487:325–329 [PubMed: 22763456]
23. Dewald O, Frangogiannis NG, Zoerlein MP, Duerr GD, Taffet G, Michael LH, Welz A, Entman ML. A murine model of ischemic cardiomyopathy induced by repetitive ischemia and reperfusion. Thorac Cardiovasc Surg. 2004;52:305–311 [PubMed: 15470614]
24. Thackeray JT, Derlin T, Haghikia A, Napp LC, Wang Y, Ross TL, Schafer A, Tillmanns J, Wester HJ, Wollert KC, Bauersachs J, Bengel FM. Molecular imaging of the chemokine receptor cxcr4 after acute myocardial infarction. JACC Cardiovasc Imaging. 2015;8:1417–1426 [PubMed: 26577262]
25. Teague HL, Ahlman MA, Alavi A, Wagner DD, Lichtman AH, Nahrendorf M, Swirski FK, Nestle F, Gelfand JM, Kaplan MJ, Grinspoon S, Ridker PM, Newby DE, Tawakol A, Fayad ZA, Mehta NN. Unraveling vascular inflammation: From immunology to imaging. J Am Coll Cardiol. 2017;70:1403–1412 [PubMed: 28882238]
26. Lewis AJM, Miller JJ, Lau AZ, Curtis MK, Rider OJ, Choudhury RP, Neubauer S, Cunningham CH, Carr CA, Tyler DJ. Noninvasive immunometabolic cardiac inflammation imaging using hyperpolarized magnetic resonance. Circ Res. 2018;122:1084–1093 [PubMed: 29440071]
27. Reiter T, Kircher M, Schirbel A, Werner RA, Kropf S, Ertl G, Buck AK, Wester HJ, Bauer WR, Lapa C. Imaging of c-x-c motif chemokine receptor cxcr4 expression after myocardial infarction

with [(68)ga]pentixafor-pet/ct in correlation with cardiac mri. JACC Cardiovasc Imaging. 2018;11:1541–1543. [PubMed: 29454781]

28. Lapa C, Reiter T, Werner RA, Ertl G, Wester HJ, Buck AK, Bauer WR, Herrmann K. [(68)ga]pentixafor-pet/ct for imaging of chemokine receptor 4 expression after myocardial infarction. JACC Cardiovasc Imaging. 2015;8:1466–1468 [PubMed: 26699115]
29. Lapa C, Reiter T, Li X, Werner RA, Samnick S, Jahns R, Buck AK, Ertl G, Bauer WR. Imaging of myocardial inflammation with somatostatin receptor based pet/ct - a comparison to cardiac mri. Int J Cardiol. 2015;194:44–49 [PubMed: 26005805]
30. Thackeray JT, Bankstahl JP, Wang Y, Korf-Klingebiel M, Walte A, Wittneben A, Wollert KC, Bengel FM. Targeting post-infarct inflammation by pet imaging: Comparison of (68)ga-citrate and (68)ga-dotatate with (18)f-fdg in a mouse model. Eur J Nucl Med Mol Imaging. 2015;42:317–327 [PubMed: 25112398]
31. Ye YX, Basse-Lusebrink TC, Arias-Loza PA, Kocoski V, Kampf T, Gan Q, Bauer E, Sparka S, Helluy X, Hu K, Hiller KH, Boivin-Jahns V, Jakob PM, Jahns R, Bauer WR. Monitoring of monocyte recruitment in reperfused myocardial infarction with intramyocardial hemorrhage and microvascular obstruction by combined fluorine 19 and proton cardiac magnetic resonance imaging. Circulation. 2013;128:1878–1888 [PubMed: 24025595]
32. Libby P, Hansson GK. Inflammation and immunity in diseases of the arterial tree: Players and layers. Circ Res. 2015;116:307–311 [PubMed: 25593275]
33. Mann DL. Innate immunity and the failing heart: The cytokine hypothesis revisited. Circ Res. 2015;116:1254–1268 [PubMed: 25814686]
34. Ridker PM. From c-reactive protein to interleukin-6 to interleukin-1: Moving upstream to identify novel targets for atheroprotection. Circ Res. 2016;118:145–156 [PubMed: 26837745]
35. Ridker PM, MacFadyen JG, Everett BM, Libby P, Thuren T, Glynn RJ. Relationship of c-reactive protein reduction to cardiovascular event reduction following treatment with canakinumab: A secondary analysis from the cantos randomised controlled trial. Lancet. 2018;391:319–328 [PubMed: 29146124]
36. Ridker PM, Everett BM, Thuren T, MacFadyen JG, Chang WH, Ballantyne C, Fonseca F, Nicolau J, Koenig W, Anker SD, Kastelein JJP, Cornel JH, Pais P, Pella D, Genest J, Cifkova R, Lorenzatti A, Forster T, Kobalava Z, Vida-Simiti L, Flather M, Shimokawa H, Ogawa H, Dellborg M, Rossi PRF, Troquay RPT, Libby P, Glynn RJ. Antiinflammatory therapy with canakinumab for atherosclerotic disease. N Engl J Med. 2017;377:1119–1131 [PubMed: 28845751]
37. Heidt T, Courties G, Dutta P, Sager HB, Sebas M, Iwamoto Y, Sun Y, Da Silva N, Panizzi P, van der Laan AM, Swirski FK, Weissleder R, Nahrendorf M. Differential contribution of monocytes to heart macrophages in steady-state and after myocardial infarction. Circ Res. 2014;115:284–295 [PubMed: 24786973]
38. Thackeray JT, Bengel FM. Molecular imaging of myocardial inflammation with positron emission tomography post-ischemia: A determinant of subsequent remodeling or recovery. JACC Cardiovasc Imaging. 2018;11:1340–1355 [PubMed: 30190033]
39. Clemente-Casares X, Hosseinzadeh S, Barbu I, Dick SA, Macklin JA, Wang Y, Momen A, Kantores C, Aronoff L, Farno M, Lucas TM, Avery J, Zarrin-Khat D, Elsaesser HJ, Razani B, Lavine KJ, Husain M, Brooks DG, Robbins CS, Cybulsky M, Epelman S. A cd103(+) conventional dendritic cell surveillance system prevents development of overt heart failure during subclinical viral myocarditis. Immunity. 2017;47:974–989.e978 [PubMed: 29166591]

NOVELTY AND SIGNIFICANCE

What Is Known?

- CCR2+ monocytes and macrophages, recruited to the site of myocardial injury, are important mediators of heart failure pathogenesis and potential therapeutic targets to improve outcomes following myocardial infarction.
- There is a lack of clinical imaging tools to noninvasively visualize inflammatory monocyte and macrophage recruitment to the injured heart.
- PET imaging using ^{64}Cu radiolabeled CCR2-binding peptide ECL1i has shown sensitivity and specificity for detecting tissue CCR2+ cells in non-cardiac mouse models.

What New Information Does This Article Contribute?

- The CCR2 targeting agent ^{68}Ga-DOTA-ECL1i demonstrated sensitive and specific detection of CCR2+ monocytes and CCR2+ macrophages in diphtheria toxin and ischemia reperfusion injury mouse models, by identifying the recruitment of CCR2+ monocytes and accumulation of CCR2+ macrophages in the injured heart.
- The heart uptake of ^{68}Ga-DOTA-ECL1i not only showed a close correlation with inflammatory chemokines and cytokines, but also was associated with indices of left ventricle function and infarct size.
- Autoradiography demonstrated specific binding of ^{68}Ga-DOTA-ECL1i to human heart failure tissues. The extent of ^{68}Ga-DOTA-ECL1i activity was associated with CCR2+ macrophage abundance.
- ^{68}Ga-DOTA-ECL1i has desirable physical properties (radiochemistry and short half-life) and pharmacokinetics to support serial PET.
- Collectively, these findings highlight the potential of ^{68}Ga-DOTA-ECL1i PET to noninvasively and serially visualize inflammatory monocyte recruitment and macrophage accumulation in the mouse and human hearts.

The heart contains distinct macrophage populations with differing origins and divergent functions. Among these subsets, CCR2+ macrophages are a particularly inflammatory population derived from circulating blood monocytes that infiltrate the heart following various forms of tissue injury and contribute to adverse cardiovascular outcomes. However, no technique is currently available to detect these cells in the heart in intact organisms. We developed and validated a molecular imaging agent to specifically visualize CCR2+ monocytes and macrophages in the mouse and human heart using positron emission tomography. These findings provide the requisite pre-clinical data needed to support clinical and translational studies focused on investigating the dynamics and prognostic implications of CCR2+ monocyte and macrophage accumulation in the heart across the spectrum of cardiac pathologies. This novel imaging technique will provide new insights into the role of inflammation during human heart failure

progression. Moreover, this technique has the potential to identify patients that may be best suited for immunomodulatory therapies.

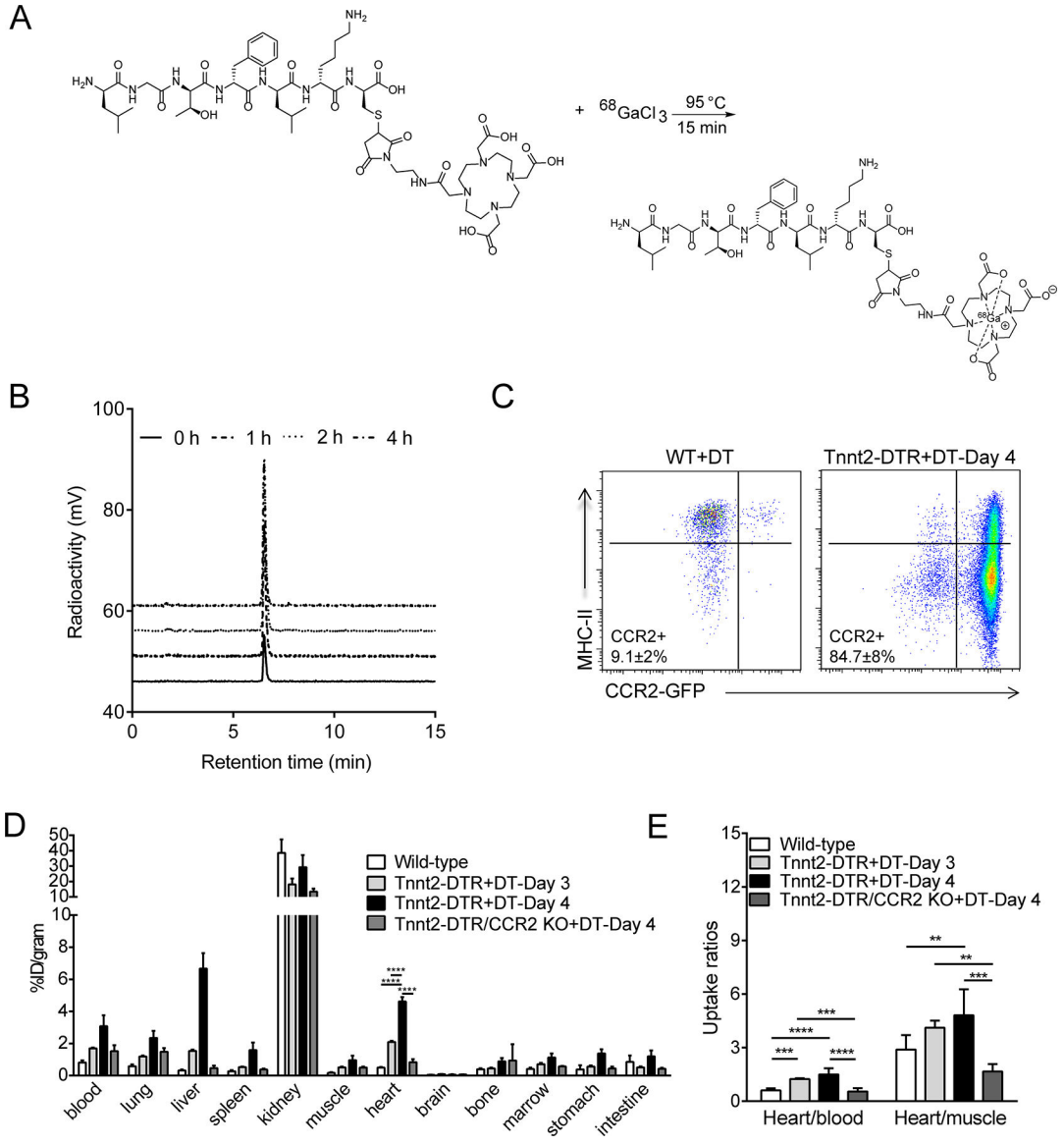

Figure 1. Generation of a CCR2-targeted ^{68}Gallium PET tracer.

(A) Synthetic scheme utilized to generate ^{68}Ga-DOTA-ECL1i. **(B)** Serum stability of ^{68}Ga-DOTA-ECL1i administered to mice via tail vein injection. **(C)** Flow cytometry showing that CCR2+ monocytes (CCR2+MHC-II^{low}) and CCR2+ macrophages (CCR2+MHC-II^{high}) accumulate in the hearts of Tnnt2-DTR mice 4 days after the administration of diphtheria toxin (DT, 25 ng IP). In contrast, the hearts of littermate control mice contain predominately CCR2- macrophages following DT injection. **(D)** Biodistribution of ^{68}Ga activity in DT treated wild type (WT) and Tnnt2-DTR mice 1 h post intravenous injection (tail vein) of ^{68}Ga-DOTA-ECL1i. n=5 per experimental group. **(E)** Tracer uptake ratios (heart/blood and heart/muscle) in WT and Tnnt2-DTR mice demonstrating enrichment of ^{68}Ga activity in the hearts of Tnnt2-DTR mice administered DT over the blood pool. n=5 per experimental group. * p< 0.05, ** p< 0.01, *** p< 0.005, **** p<0.001.

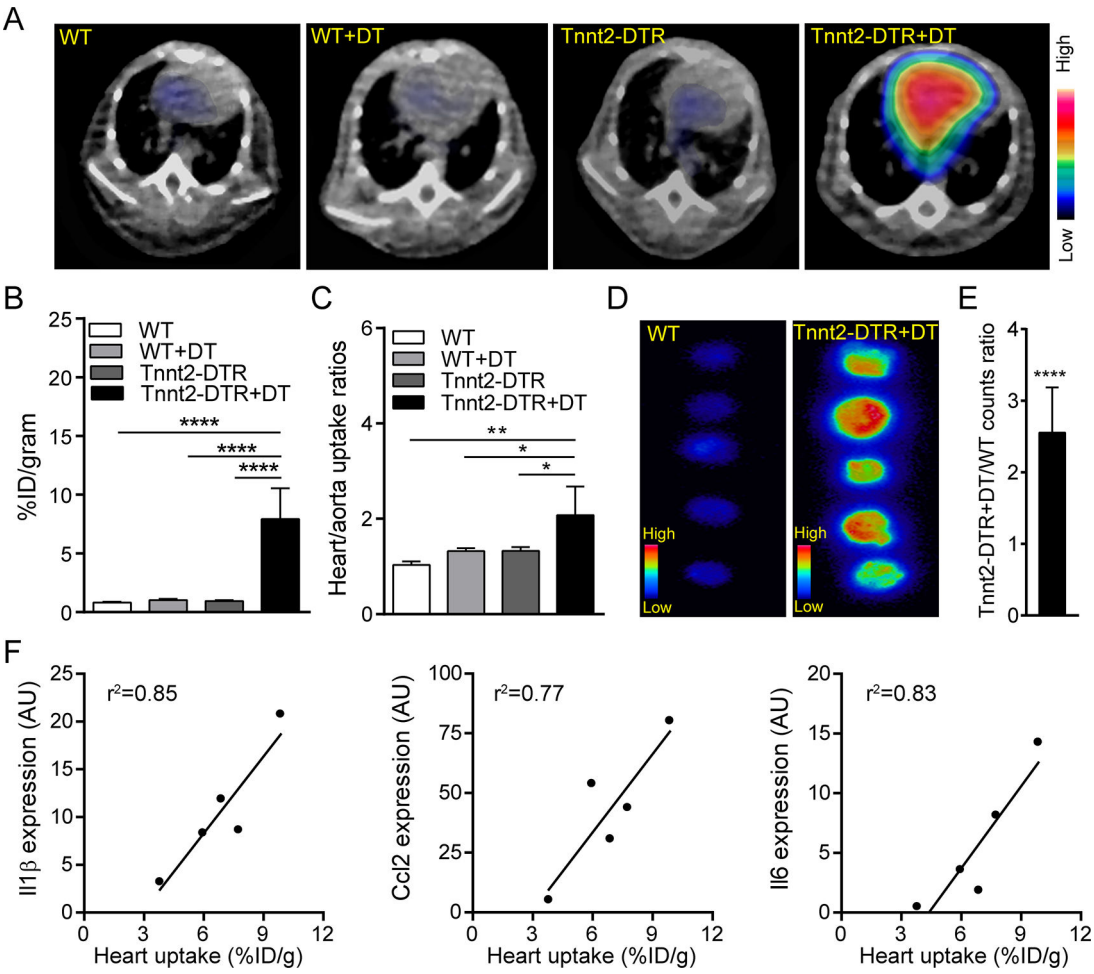

Figure 2. PET of ^{68}Ga-DOTA-ECL1i in a mouse model of cardiomyocyte ablation.

(A) Representative PET/CT images of ^{68}Ga-DOTA-ECL1i in wild-type (WT) and Tnnt2-DTR mice 4 days following either vehicle (PBS) or diphtheria toxin (DT) administration. Arrow denotes robust tracer accumulation in the hearts of Tnnt2-DTR+DT mice compared to all other groups. PET images are overlaid on CT images. **(B)** Quantitative analysis of ^{68}Ga-DOTA-ECL1i signal in the hearts of WT and Tnnt2-DTR mice treated with either vehicle or DT. n=5 per experimental group. **(C)** Ratio of ^{68}Ga-DOTA-ECL1i signal between the heart and aorta of WT and Tnnt2-DTR mice demonstrating that increased ^{68}Ga-DOTA-ECL1i signal in Tnnt2-DTR+DT hearts is not a result of increased blood pool signal, n=5 per experimental group. **(D)** Autoradiography of heart slices collected from WT and Tnnt2-DTR mice immediately after PET showing myocardial uptake of ^{68}Ga-DOTA-ECL1i. Mice were flushed with saline prior to heart collection and autoradiography to remove intravascular cells. **(E)** Quantitative comparison of radioactivity measured from autoradiography images of WT and Tnnt2-DTR hearts expressed as fold increase over WT control. **(F)** Linear regression of ^{68}Ga-DOTA-ECL1i heart uptake and chemokine/cytokine mRNA expression. n=5 per experimental group. * $p< 0.05$, ** $p< 0.01$, *** $p< 0.005$, **** $p<0.001$.

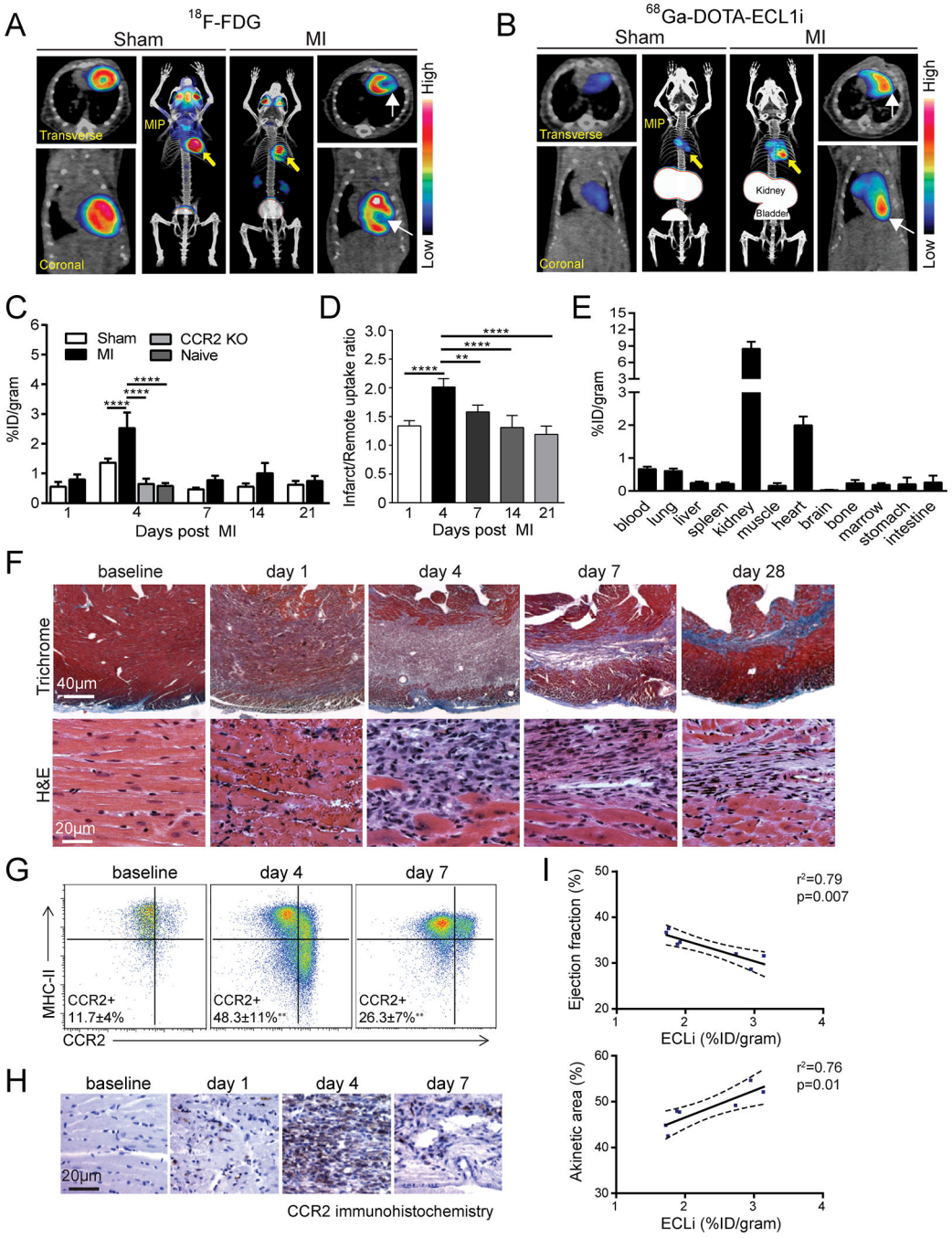

Figure 3. PET of ^{68}Ga-DOTA-ECL1i in a mouse model of closed-chest ischemia reperfusion injury.

(A) Representative ^{18}F-FDG PET/CT images obtained 5 days following 90 minutes of ischemia reperfusion injury identifying the infarct region in mice that underwent ischemia reperfusion injury (MI) compared to sham controls. Transverse, coronal, and maximal intensity projected (MIP) views are shown and white arrows denote the infarct area. **(B)** Representative ^{68}Ga-DOTA-ECL1i PET/CT images showing regional accumulation of ^{68}Ga-DOTA-ECL1i signal in the infarct and border zone 4 days following ischemia reperfusion

injury. Transverse, coronal and maximal intensity projected (MIP) views are shown. Yellow arrow identifies tracer uptake in hearts that underwent ischemia reperfusion injury compared to sham controls. White arrows denote the infarct area as determined by ^{18}F-FDG imaging. **(C)** Quantitative analysis of ^{68}Ga-DOTA-ECL1i accumulation in the hearts of naïve, sham, MI, and CCR2 KO mice that underwent ischemia reperfusion injury at the indicated time points. n=4–5 per experimental group. **(D)** Regional accumulation of ^{68}Ga-DOTA-ECL1i uptake in the infarct and remote areas of sham and MI mice over the indicated time points. **(E)** Biodistribution of ^{68}Ga activity 4 days following ischemia rerpefusion injury measured 1 h post intravenous injection (tail vein) of ^{68}Ga-DOTA-ECL1i. n=5 per experimental group. **(F)** Trichrome and H&E staining show the evolution of fibrosis (trichrome-blue, 40X magnification) and cell infiltration (H&E, 200X magnification) over time in the closed-chest ischemia reperfusion injury model. Note the dense accumulation of cells within the infarct 4 days following ischemia reperfusion injury. Representative images from 6 independent experiments. **(G)** Flow cytometry analysis showing accumulation of CCR2+ monocytes (CCR2+MHC-II^{low}) and CCR2+ macrophages (CCR2+MHC-II^{high}) 4 days following ischemia reperfusion injury and persistence of CCR2+ macrophages 7 days following ischemia reperfusion injury compared to sham controls. **(H)** Immunostaining showing accumulation of CCR2+ cells (brown) in the infarct region peaking at day 4 following ischemia reperfusion injury. **(I)** Linear regression analyses showing the relationship between ^{68}Ga-DOTA-ECL1i heart uptake measured on day 4 following ischemia reperfusion injury and echocardiographic assessment of LV ejection fraction and akinetic area measured on day 28 following ischemia reperfusion injury. * $p< 0.05$, ** $p< 0.01$, *** $p< 0.005$, **** $p<0.001$.

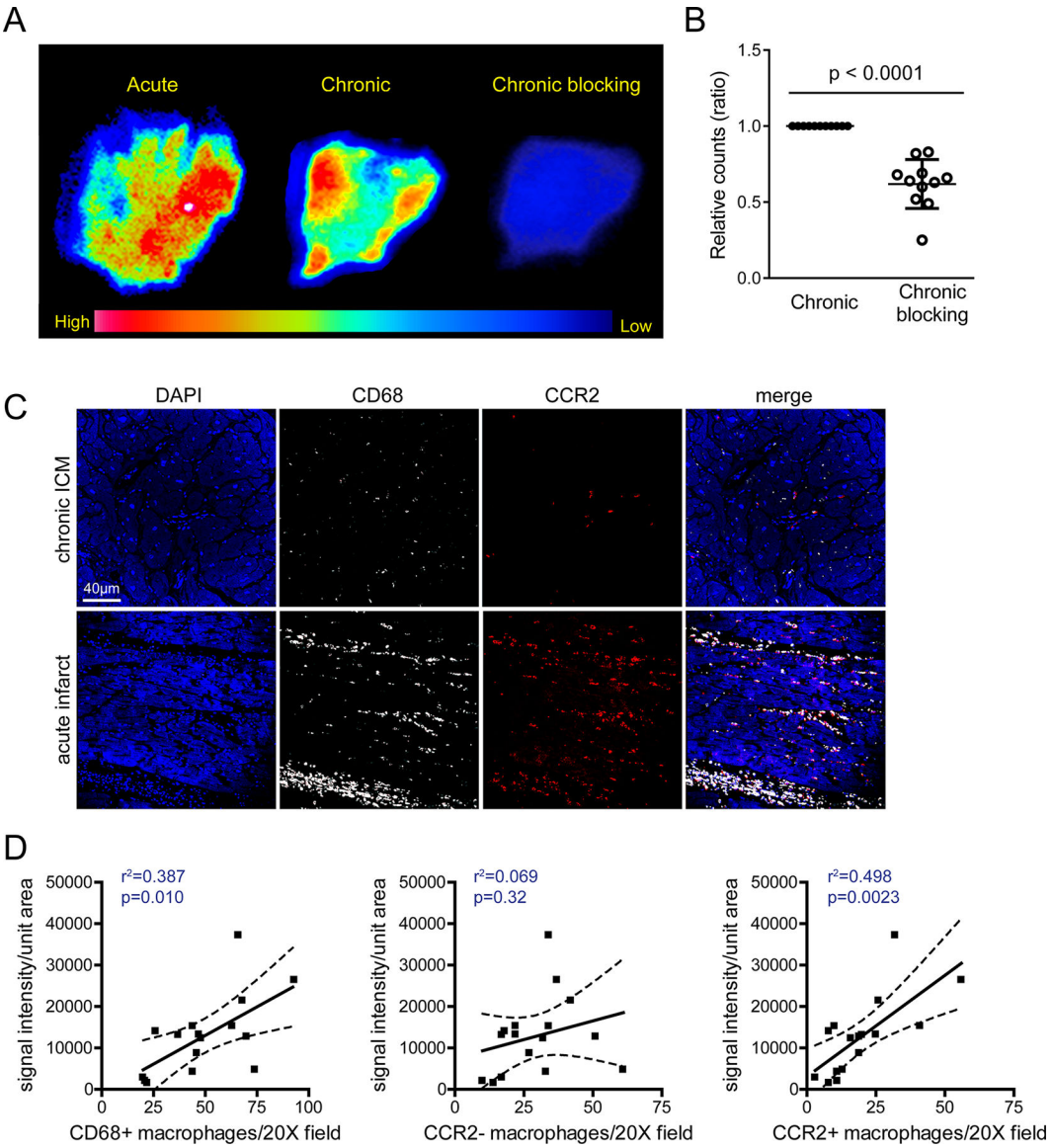

Figure 4. ^{68}Ga-DOTA-ECL1i identifies CCR2+ monocytes and macrophages in the human heart.

(A) Autoradiography images of human acute myocardial infarction and chronic ICM specimens incubated with ^{68}Ga-DOTA-ECL1i revealing heterogeneous distribution or tracer binding. Competitive blocking assaying using excess non-radioactive DOTA-ECL1i showing decreased tracer binding. **(B)** Quantification of ^{68}Ga-DOTA-ECL1i binding (displayed as relative counts ratio) demonstrated significantly decreased tracer binding following co-incubation with DOTA-ECL1i blocking agent (n=11). **(C)** Immunohistochemical staining for CD68 (white), CCR2 (red), and DAPI (blue) highlighting the distribution of CCR2-CD68+ and CCR2+CD68+ macrophages in human ICM samples. Representative images (200X magnification) from acute ICM (n=5) and chronic ICM (n=11) samples. **(D)** Linear regression analysis demonstrating that the intensity of ^{68}Ga-DOTA-ECL1i binding is associated with the number of total CD68+ macrophages (left) and abundance of CCR2+ macrophages (right). No association was detected between ^{68}Ga-DOTA-ECL1i binding and

the number of CCR2- macrophages (center). * p< 0.05, ** p< 0.01, *** p< 0.005, **** p<0.001.